Journal of Engineering Science and Technology
Vol. 12, No. 6 (2017) 1460 - 1474

EMBEDDED CONTROLLER BUILDING FOR BALL AND BEAM SYSTEM USING OPTIMAL CONTROL SYNTHESIS

B. M. HUNG[1], S. S. YOU[1,*], H. S. KIM[2], T. W. LIM[3]

[1]Division of Mechanical Engineering, Korea Maritime and Ocean University, Busan, Korea
[2]Division of Logistics Engineering, Korea Maritime and Ocean University, Busan, Korea
[3]Division of Marine Engineering, Korea Maritime and Ocean University, Busan, Korea
*Corresponding Author: ssyou@kmou.ac.kr

Abstract

The controller design for the Ball and Beam system is particularly crucial in the aviation fields due to its likeness to the aircraft control during the flight and landing under turbulent. Since the actual tests on the aircrafts are not possible, the Ball and Beam system could be necessary as an alternative to these manoeuvring. In addition, the ball and beam system is a nonlinear dynamical model intended to test various control algorithms. The complete system includes a ball, a beam, a motor and several sensors. The input torque is generated from the motor to control the position of the ball on the beam, where the ball rolls on the beam freely. The concise mathematical model has been obtained by linearized around the horizontal region. The presented control strategies are based on the optimal control synthesis including LQR and H_2 optimization to manipulate the complete ball-beam system. These control algorithms have been successfully tested to figure out the control performance for specific applications. Finally, the control systems are implemented in the real ball and beam system with a data acquisition card of DSP F28335.

Keywords: Ball and beam system, Linear quadratic regulator (LQR), Linear quadratic Gaussian (LQG), H_2 optimization.

1. Introduction

The ball and beam system is a typical mechatronics system for controller analysis. It consists of a rigid beam which is freely rotated in the vertical plane at the pivot while a ball rolls along the beam. It can be categorized into two configurations. The first configuration is normally called the ball and beam balancer, in which the beam is simply supported in the middle, and rotates about its central axis. The

Nomenclatures

B_m	Viscous friction coefficient
d	Lever's arm offset, m
g	Gravitational acceleration, $\mathrm{m/s^2}$
I_m	Armature current, A
J_m	Effective moment of inertia, $\mathrm{kg.\,m^2}$
J_Δ	Quality criteria
K_b	Back electromotive force constant, $\mathrm{V/rad/s}$
K_m	Torque constant, $\mathrm{Nm/A}$
L	Beam length of the beam, m
L_m	Inductance of the armature, H
m	Ball mass, kg
M	Beam mass, kg
r	Ball position, m
R_m	Armature resistance, Ω
τ_m	Torque acting on the beam, $\mathrm{N.\,m}$

Greek Symbols

α	Beam angle, rad
θ	Servo gear angel, rad
ψ	Function of state variable x

Abbreviations

DSP	Digital Signal Processing
DC	Direct Current
LQG	Linear Quadratic Gaussian
LQR	Linear Quadratic Regulator
PID	Proportional Integral Derivative

advantage of this form is that it is easy to build the model, and the corresponding mathematical model is relatively simple. The second configuration is constructed with the beam supported on both sides by two level arms. One of the level arms provides the pivot, and the other is coupled to the motor output gear. The disadvantage is that it requires more consideration for the mechanical parts, which imposed some difficulties on deriving a mathematical model. The aim of the ball and beam system is to position the ball at a desired location on the beam. The ball position cannot be controlled directly, but only through beam angle. Thus, it will imply the presence of the two integrators plus the dynamical properties of the beam. This fact results in imposing an open loop unstable problem.

Many studies have been made on the ball and beam system related to the first configuration. Hirsch [1] built the ball on the beam system with the first configuration, which was implemented with an ultrasonic sensor to measure the position of the ball. The beam angle was measured through a potentiometer. The motor with gearbox was driven with a high power op-amp circuit. The applied controller is a PD-type synthesis which shows the response with the settling time of about 150ms. However, there exist some steady state errors most likely due to the ignorance of the friction in the system. Rosales [2] built the ball and beam system which is made of acrylic with the first configuration. This system used a

linear potentiometer technique for monitoring the ball position on the beam and the encoder sensor to measure the angle of the beam. In this model, the ball position is controlled by an inner motor loop and an outer ball position loop using a dSPACE controller board. As expected, the ball could be balanced at any position along the beam. The experimental results show that the ball with small step commands tracked the position quickly without overshooting. However, the ball tended to either overshot and oscillated several times before coming to rest, or to become unstable and lose system equilibrium. Lieberman [3] built a system named a robotic ball balancing beam with the first configuration. The system is similar to the ball on beam system developed by Hirsch [1]. The only difference between two systems is that Lieberman [3] used a resistive wire position sensor while Hirsch [1] used an ultrasonic position sensor. In this system, the test results on the P-type controller showed that the response is not only stable but also reasonably fast and almost critically damped. In reality, the system response of ball position showed a modest overshoot.

Quanser [4] presented the commercial product named the ball and beam module with the second configuration. This module consisted of the position sensors made of resistive wires and a DC servo motor with gearbox reduction. The PID and state-space control method have been applied to balance the ball on the beam. This system can control the ball position at any point on the beam. When the input or output signal has little noise or disturbance, then the ball jump up, and the system loses the ball information. Another control algorithm which made this kind of system more stable by using the truncated back propagation through time with the node –decoupled extended Kalman filter (NDEKF) algorithm to update the weights in the networks of neuro controller. This system is designed by Eaton [5], then implemented in the ordinary and fuzzy ball and beam model. Generally, the results so that the adaptive critic-based controller has the performance which is better than the performance of the conventional controller.

Recently, the second configuration model is also developed and implemented. Ezzabi et al. [6] designed this kind of model using the backstepping algorithm. The results show that the nonlinear backstepping design gives a smoother performance and steady state responses. Using the same kind of model, Pang et al. [7] has proposed an STF-LQR control strategy for the ball and beam system. The linearized augmented state space model can be estimated online by using STF. However, the controller cannot ensure the good responses in the noisy environment. Yu [8] uses PD controller to control a nonlinear ball and beam system model. This controller has used Lyapunov's direct method for well-defined set of initial conditions. The results show that the system can due with the disturbance and stable.

This paper deals with the optimal control synthesis LQR and $H_{2/\infty}$ follows Doyle et al. [9] and [10], which can enhance the system performance by eliminating the disturbance or noise. The unique features of the presented ball-on-beam system are as follows. First, it employs an inexpensive and mechanically simple mechanism which consists of a servo motor, a position sensor, amplifier circuits, a DSP board, an aluminum beam, and some mechanical parts. Second, the sensing of the ball position can be made only by using distance sensors. Third, it utilizes a DSP TMS320F2833 for the control algorithm implementation which

enjoys all of the convenience features that come with DSP board. In particular, changing the control algorithms is simply done by flashing the codes for the control methods into the DSP TMS F28335, without changing the hardware. Finally, the dynamic responses for the reference tracking have been presented to verify the effectiveness of the proposed approach.

2. Mathematical Modelling of The Ball and Beam System

As shown in Fig. 1, the mechanical configuration of ball and beam system is the same as Keshmiri et al. [11], which consists of five main components: the ball, the beam, two mechanical arms, the gear, and the DC servo motor. The beam motion is manipulated by the DC servo motor with the ball rolling back and forth on the beam track.

The ball is placed on a beam, in which the ball rolls freely along the beam's horizontal plane. The lever arm is attached to the beam at one end and the servo gear at the other. As the servo gear turns, the lever changes the beam angle α. The force that accelerates the ball comes from the component of gravity. The ball actually goes along the beam by rolling and sliding without friction.

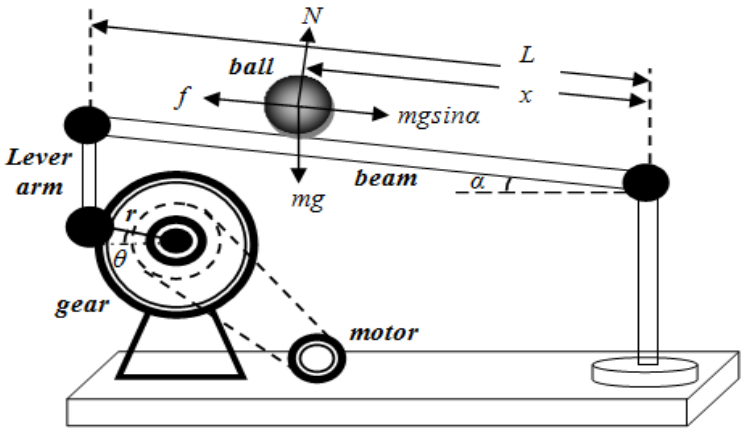

Fig. 1. The complete ball and beam system.

The mathematical modeling of the complete system includes the DC servo motor dynamics, kinematics relationship on α and the servo gear angle θ, and ball dynamics along with the beam. Based on Kirchoff's voltage law, the DC motor equation is given as follows

$$V_{in} = I_m R_m + K_b \dot{\theta} + L_m \frac{di}{dt} \quad (1)$$

where V_{in} is the input voltage, I_m is an armature current, R_m and L_m are the resistance and inductance of the armature, K_b is back e.m.f constant in the DC motor circuit, and $\dot{\theta}$ is the angular velocity. Since the inductance of the armature is relatively small, the DC motor Eq. (1) can be simplified in Eq. (2)

$$V_{in} = I_m R_m + K_b \dot{\theta} \quad (2)$$

Then the torque acting on the beam is described by

$$\tau_m = \frac{1}{K_g}\left(J_m\ddot{\theta} + B_m\dot{\theta}\right) = K_m I_m \tag{3}$$

where B_m is the viscous friction coefficient, τ_m is the rotational force (or torque) of the motor, K_g is the gear ratio of the motor's shaft and servo gear, J_m is the effective moment of inertia, and K_m is the torque constant of the motor. As a result, the DC motor model is further calculated by

$$V_{in} = \frac{R_m J_m}{K_m K_g}\ddot{\theta} + \left(K_b + \frac{R_m B_m}{K_m K_g}\right)\dot{\theta} \tag{4}$$

In the absence of friction or other disturbances, the complete dynamics of the ball on a beam system can be obtained by Lagrangian method

$$H = T - P = \frac{1}{2}\left[(J_1 + mr^2)\dot{\alpha}^2 + \frac{7}{5}m\dot{r}^2\right] - \left(mgr + \frac{L}{2}Mg\right)sin\alpha \tag{5}$$

where the Lagrangian H of a mathematical function summarizes the dynamics of the system. Since there is no external force on the ball in the radial direction, the Lagrange equations of motion are given in Eq. (6)

$$\begin{cases}(J_1 + mr^2)\ddot{\alpha} + 2mr\dot{r}\dot{\alpha} + \left(mgr + \frac{L}{2}Mg\right)cos\alpha = \tau \\ \frac{7}{5}\ddot{r} - r\dot{\alpha}^2 + gsin\alpha = 0\end{cases} \tag{6}$$

By assuming that the beam angle is very small without friction, it leads to $gsin\alpha \approx g\alpha$. Then linearizing these equations can be estimated when the system approaches the stable point. At this point $\dot{\alpha} \approx 0$, then the term $-r\dot{\alpha}^2 \approx 0$. Equation (6) becomes

$$\begin{cases}(mr^2 + K_1)\ddot{\alpha} + (2mr\dot{r} + K_2)\dot{\alpha} + \left(mgr + \frac{L}{2}Mg\right)cos\alpha = \tau \\ K_4\ddot{r} - r\dot{\alpha}^2 + g\alpha = 0\end{cases} \tag{7}$$

where

$$K_1 = \frac{R_m J_m L}{K_m K_g d} + J_1; K_2 = \frac{L}{d}\left(\frac{K_m K_b}{R_m} + K_b + \frac{R_m B_m}{K_m K_g}\right); K_3 = 1 + \frac{K_m}{R_m};$$

$$K_4 = \frac{7}{5};\ \tau = K_3 V_{in} \tag{8}$$

The model can be described by the state equation form using the following notation: x_1 for ball position along the beam with $x_1 = r(m)$; x_2 for ball velocity with $x_2 = \dot{r}\left(\frac{m}{s}\right)$; x_3 for beam angle with $x_3 = \alpha(rad)$, and $x_4 = \dot{\alpha}\ (\frac{rad}{s})$ for beam angular velocity. Consequently, the complete state equations are given by Eq. (9)

$$\begin{cases}\dot{x}_1 = x_2 \\ \dot{x}_2 = -\frac{g}{K_4}x_3 \\ \dot{x}_3 = x_4 \\ \dot{x}_4 = \frac{1}{(mx_1^2 + K_1)}\left[K_3 V_{in} - (2mx_1x_2 + K_2)x_4 - \left(mgx_1 + \frac{L}{2}Mg\right)cos\, x_3\right]\end{cases} \tag{9}$$

3. Optimal Control Synthesis

3.1. LQR controller design

Considering the state-space representation of the system with input force $u \neq 0$. The most important step for an optimal control is to define the quality criterion J_Δ. This criterion depends on the system output, the control signal, and the time. Then the optimal control problem is to determine the control input *u(t)* that makes the optimal criteria J_Δ to reach extreme values within the limit conditions of *u* and *x*. The criteria has the form as Eq. (10)

$$J_\Delta = \int_0^T \psi[x(t), u(t), t]dt \tag{10}$$

where ψ is a function of state variable x, control input u and the time t. The LQR problem is to determine a control sequence u_k^*, $k > 0$ which minimizes the following cost function

$$J_\Delta = \int_0^\infty [x^T Q x + u^T R u]dt \tag{11}$$

where Q is a symmetric positive semidefinite weighting matrix, and R is a symmetric positive definite weighting matrix. The control input with state feedback is given in Eq. (12)

$$u(t) = -Kx(t) \tag{12}$$

where K is a controller gain. This feedback matrix can be calculated as $K = R^{-1}B^T S$ using $A^T S + SA - SBR^{-1}B^T S + Q = -\dot{S}$. When S is independent of time, i.e., $\dot{S} = 0$, the Riccati equation is given in Eq. (13)

$$A^T S + SA - SBR^{-1}B^T S + Q = 0 \tag{13}$$

For a discrete- time system, the state-space representation is described by

$$x_{k+1} = A_k x_k + B_k u_K \tag{14}$$

where $x_k \in R^n$ and $u_k \in R^m$. Finally, the control law is determined by $u_k = -K_k x_k$, where the coefficient K_k can be calculated by Eq. (15)

$$K_k = (B_k^T S_{k+1} B_k + R_k)^{-1} \tag{15}$$

It is noted that S_k must satisfy the Eq. (16)

$$S_k = A_k^T \left(S_{k+1}^{-1} + B_k R_k^{-1} B_k^T\right) A_k + Q_k \tag{16}$$

3.2. Calculating the feedback gain (K)

Following the optimal control method (LQR) of Pang et al. [12], the system parameters are given as follows: $d = 0.075m$; $L = 0.7m$ and sampling frequency $T = 0.01s$. The state-space representation in the discrete–timedomain is calculated by Eq. (17)

$$\begin{cases} x(k+1) = A_D x(k) + B_D u(k) \\ y(k) = C_D x(k) + D_d u(k) \end{cases} \tag{17}$$

The transfer function of the system is described by

$$P(s) = C_D(SI - A_D)^{-1}B_D + D_D \tag{18}$$

where the system matrices are given in Eq. (19)

$$A_D = \begin{pmatrix} 1 & 0.01 & 0.0004 & 0 \\ 0 & 1 & -0.0701 & 0.0004 \\ 0 & 0 & 1 & 0.01 \\ 0 & 0 & 0 & 1 \end{pmatrix}, \; B_D = \begin{pmatrix} 0 \\ 0 \\ 0.0005 \\ 0.1083 \end{pmatrix} \tag{19}$$

$$C_D = \begin{pmatrix} 1 & 0 & 0 & 0 \\ 0 & 0 & 1 & 0 \end{pmatrix}, \qquad D_D = 0$$

The weighting matrices for the discrete Riccati equation are given as follows

$$Q = [50000 \quad 10000 \quad 1000 \quad 1], \; R = 1 \tag{20}$$

Finally, the feedback control gain is obtained by Eq. (21)

$$K = [-178.7509 \quad -151.8535 \quad 35.0073 \quad 3.6183] \tag{21}$$

To understand the processing of system clearly, the flowchart of the control algorithm is described in Fig. 2.

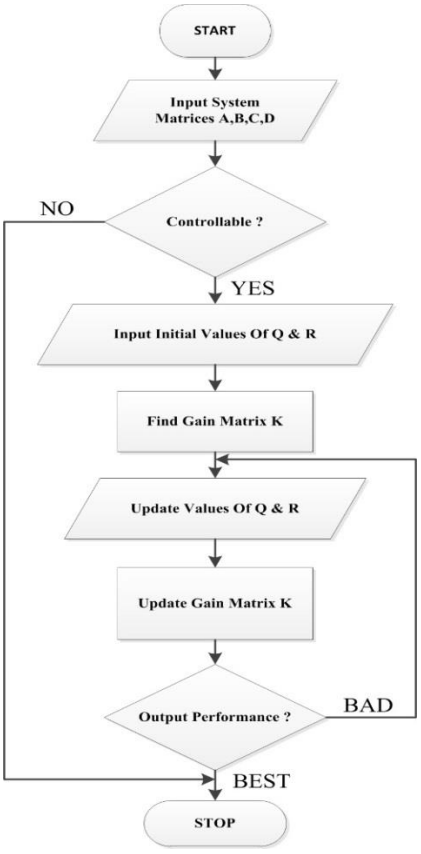

Fig. 2. The control flowchart of LQR algorithm.

3.3. Linear H_2 controller design

For the H_2 control synthesis, the control system can be analyzed in a generalized plant form. The closed loop control system with exogenous inputs w is shown in Fig. 3, where n is the measurement noise and r is the reference input.

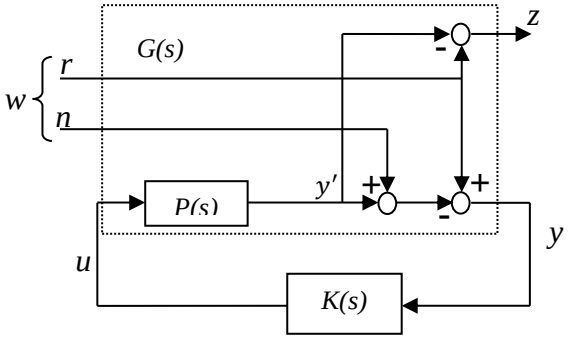

Fig. 3. The block diagram of the control system with exogenous inputs.

The generalized plant $G(s)$ of this system is described by Eq. (22)

$$\begin{bmatrix} z \\ y \end{bmatrix} = \begin{bmatrix} y' - r \\ r - y' - n \end{bmatrix} = \begin{bmatrix} Pu - r \\ r - Pu - n \end{bmatrix} = \left[\begin{array}{ccc} -I & 0 & P \\ I & -I & -P \end{array}\right] \begin{bmatrix} r \\ n \\ u \end{bmatrix} = G \begin{bmatrix} w \\ u \end{bmatrix} \tag{22}$$

The objective functions for gain matrices K is formulated using the H_2 norm from disturbance input w to state output z shown in Fig. 4. The H_2 norm is the quadratic criterion used in the optimal control as LQG. It is noted that the control structure from Fig. 3 is equivalent to the block diagram for the generalized plant described in Fig. 4.

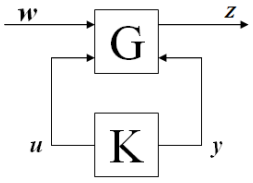

Fig. 4. Linear fractional transformation representation of control system.

In this framework, the generalized plant G has different order (McMillan number) and different number of inputs and outputs with respect to the original plant, depending on specific weighting functions and design strategies. The overall control objective is to minimize the norm of the transfer function matrix from the weighted exogenous input w to the control quality outputs z. Thus the optimization problem is given in Eq. (23)

$$\min \inf_{K \in RH_\infty} \left\| H_{w-z} \right\|_2 \tag{23}$$

where

$$H_{w-z} = F_L(G,K) = G_{11} + G_{12}K(I - KG_{21})^{-1}G_{22}, \text{ and } G = \left[\begin{array}{c|c} G_{11} & G_{12} \\ \hline G_{21} & G_{22} \end{array}\right] \quad (24)$$

It is noted that the generalized plant is partitioned according to the dimensions of *w*, *u* and *z*, *y*, respectively. The H_2 optimal control problem can be solved by observing that it is equivalent to a conventional LQG optimal control problem.

The H_2 optimal controller is thus feasible in the usual LQG manner as a full state feedback K_{CL} and gain matrix *L are* shown in Fig. 5.

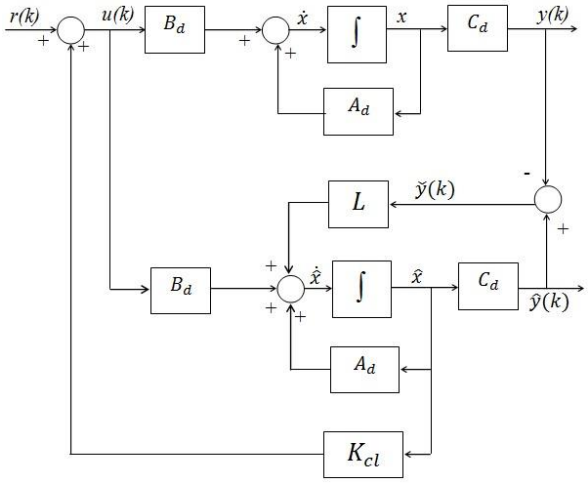

Fig. 5. The full state feedback control system.

Finally, the control gain matrix K_{CL} and the gain matrix *L* are calculated in Eq. (25)

$$\begin{cases} \dot{\hat{x}} = A_d + B_d * K_{CL} + L * C_d)\hat{x} - Ly \\ u = -K_{CL} * \hat{x} \\ K_{CL} = [-2.4448 \quad -500.1891 \quad 350.5383 \quad 5.0243] \\ L = \begin{pmatrix} 0.2101 & 1.0606 & 0.1027 & 1.7473 \\ -0.1205 & -0.8577 & 0.2760 & 2.6490 \end{pmatrix}^T \end{cases} \quad (25)$$

4. Results and Discussion

4.1. Simulation results

The simulation results for tracking control are illustrated in Fig. 6, where LQR parameters are firstly chosen as diag $Q = [50000\ 10000\ 1000\ 1]$ and $R = 1$. Figure 6(a) shows that the control outputs track the changes of the step-type reference at steady state. However, the controller gives a transient response with settling time of 3.4 seconds and rising time of 1 second. In order to meet the design criteria ensuring fast rising and settling time, the design parameter has been changed as follows: diag $Q = [500000\ 10000\ 1000\ 1]$. Now, the control performance

with new parameters (Q) provides the transient response with settling time of 1.5 seconds and rising time of 0.6 seconds without overshoot. In addition, Figure 6(b) shows the beam angle response with the old and new parameters (Q).

As illustrated in Fig. 7, it is shown that the output tracks the changes in the reference signals for a rectangular input successfully. The controller gives a good tracking performance with the settling time of 3.4 seconds and rising time of 1.2 seconds with low overshoot. The output signal with new parameters in (Q) offers the excellent transient response of settling time of 1.35 seconds and rising time of 0.6 seconds without overshoot.

Figure 8 shows the ball velocity response for the step and rectangular input. The response signals of ball velocity in two cases, Figs. 8(a) and (b) give a good performance which reduced the ball velocity from 0.78 to 0.37 (m/s). That means the control system with new parameter (Q) can balance the ball faster than the previous one.

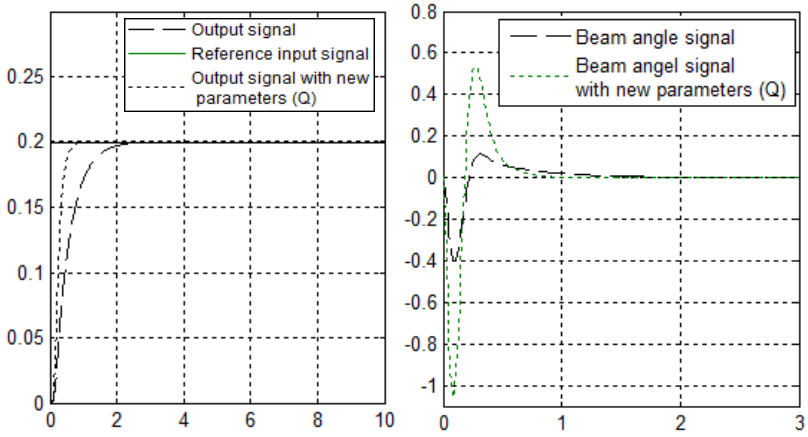

(a) Ball position **(b) Beam angle**

Fig. 6. Tracking performance with step input.

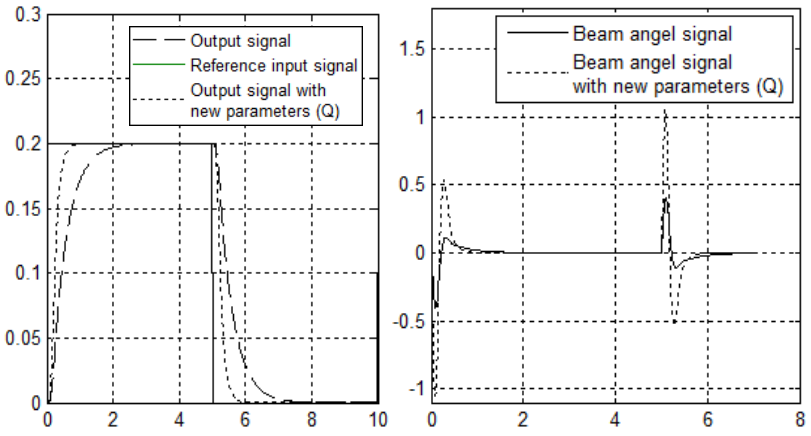

(a) Ball position **(b) Beam angle**

Fig. 7. Reference tracking with rectangular input.

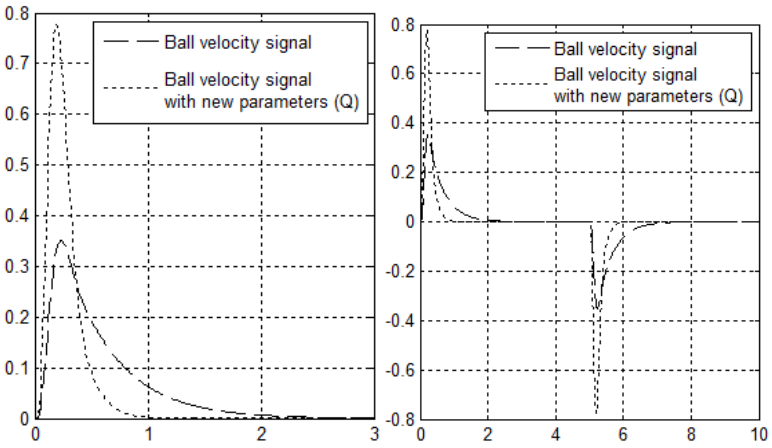

(a) Step input **(b) Rectangular input**

Fig. 8. The ball velocity with step and rectangular input.

Figure 9 provides the performance comparison between LQR, H_2 and the best-tuned PID controllers. It can be seen that LQR gives the excellent tracking response with settling time less than 0.5 seconds.

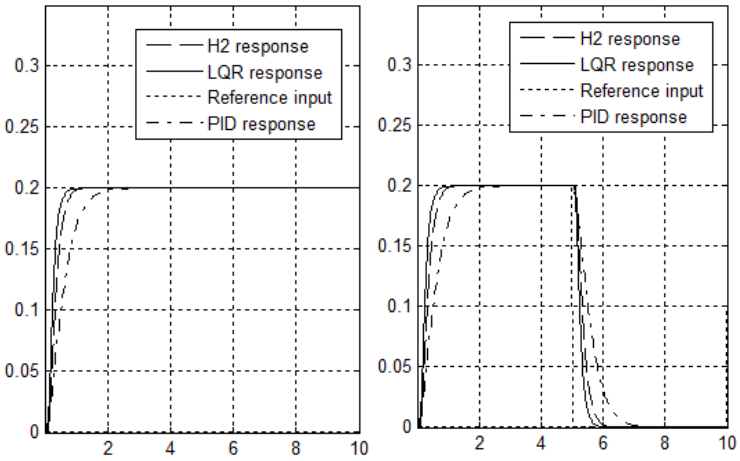

(a) Step input **(b) Rectangular input**

Fig. 9. The performance comparison between LQR, H_2 and PID without noises.

In addition, Fig. 10 illustrates the ball position signal with sensor noises using H_2 control method. Although the control system is severely affected by noise, the H_2 (LQG) controller still gives a good response with the rising time of 0.8 seconds and the settling time of 1.5 seconds without overshoot.

Figure 11 shows the ball velocity and beam angle with noises using H_2 control method. Under sensor noises at the input and output of the system, the responses for ball velocity and beam angle are still stable.

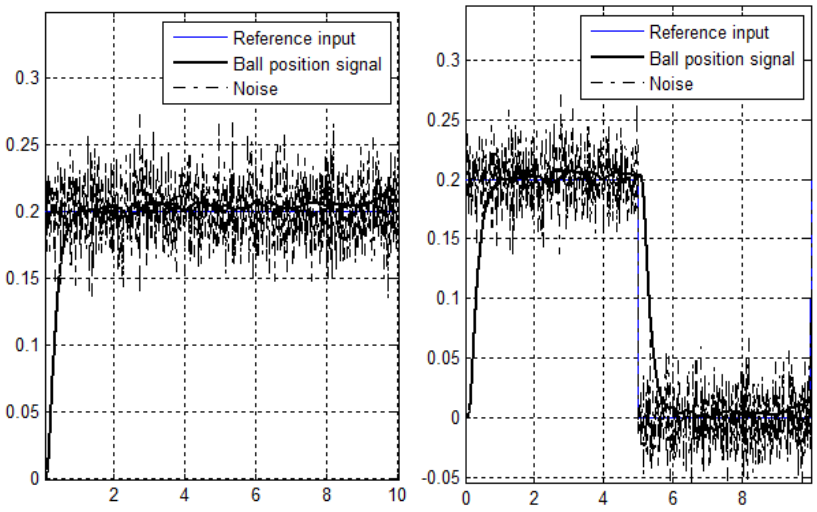

(a) Step input **(b) Rectangular input**

Fig. 10. The ball position signal with noises using H_2 control synthesis.

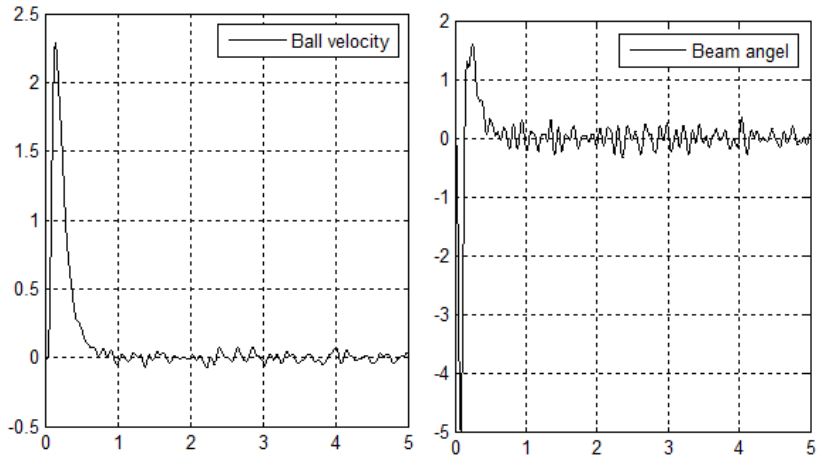

(a) Ball velocity **(b) Beam angle**

Fig. 11. The output signal with noises using H_2 control synthesis.

Generally, the simulation results show that the output signals track the reference inputs effectively. From the comparison in Fig. 9, it can be said that the PID controller offers reasonable performance, but the rising time and the settling time are also slower than those of the LQR controller. According to the characteristics of the H_2 controller, it can effectively eliminate most of the sensor noises as demonstrated in Fig. 10. The fast response is important for this system to track the changing input in time to balance the ball position on the beam. Therefore, the LQR controller is chosen to implement into the control hardware on the ball-beam system.

4.2. Experimental test results

As shown in Fig. 12, the ball and beam system with the second configuration has been built to validate the proposed LQR approach. The design parameters of the controlled mechanical system are chosen as follows: beam inertia $J = 7.3510^{-4} kg.m^2$, and ball mass $m = 0.5\,kg$. A part of the control algorithm (input calibration and filtering) has been programmed using Matlab-Simulink blocks while the control laws are programmed in C language. The designed model is complied and downloaded to the DSP. The fixed step Euler method was used for numerical integration with the sampling time of 0.01 second.

Fig. 12. The real ball and beam system.

A discrete–time LQR controller is first designed based on the simplified system Eq. (18) with the sampling period of $T_s = 0.01s$. Figure 13 illustrates that the ball position can be reached at the set position quickly. Specifically, the system gives a response with the settling time of less than 1.6 seconds and rising time of less than 1.5 seconds. In addition, Figs. 14 and 15 show that the ball approaches the desired positions (38cm and 52 cm), then remains at this point with stability. This result agreed well with simulation result shown.

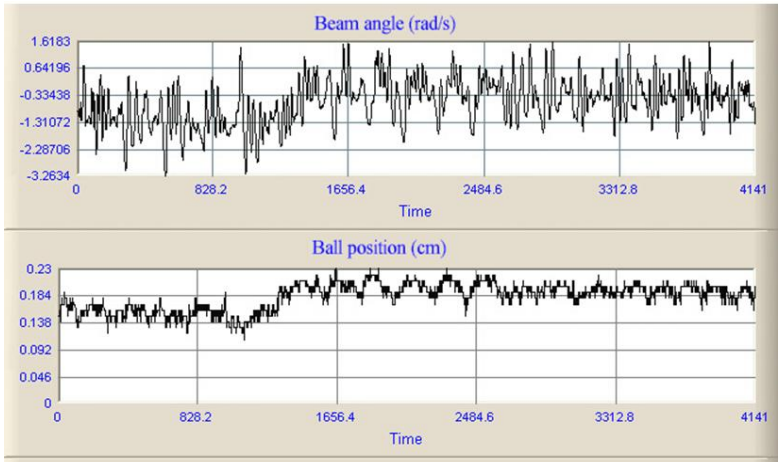

Fig. 13. LQR experiment with the position of 18 cm.

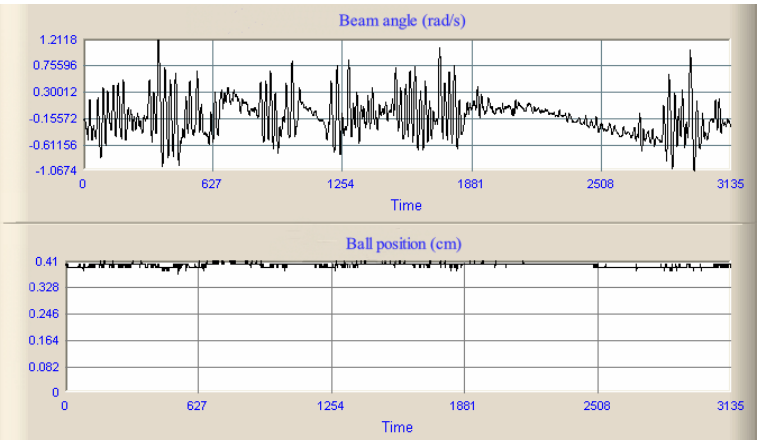

Fig. 14. LQR experiment with the position of 38 cm.

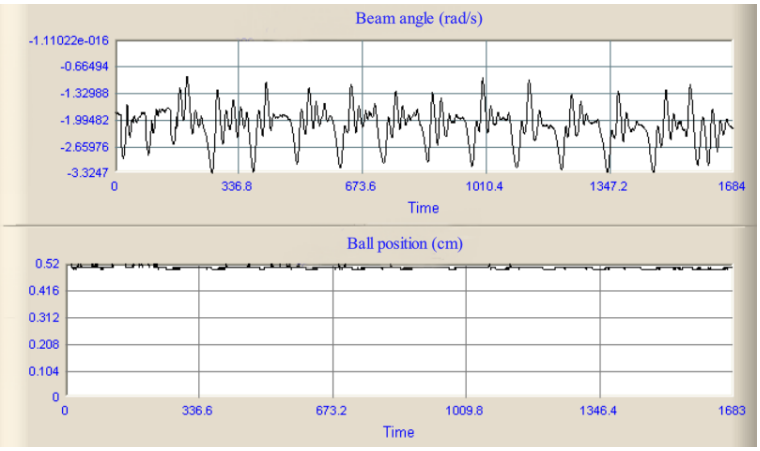

Fig. 15. LQR experiment with the position of 52 cm.

5. Conclusion

This paper deals with the mathematical model and optimal control synthesis for the ball and beam system. From the extensive simulation results, the optimal LQR scheme provides the excellent control performance for the system dynamics. Although the H_2 optimal controller offers a little slower response, it can successfully cope with most of the sensor noises encountered in the control system. For adapting the free rolling of the ball on the beam, the fast response is a critical requirement. Therefore, the LQR controller is selected to implement the experimental system, which gives the fastest response. Based on the discrete-time LQR approach, several experimental studies have been made in order to validate the presented control methods. The simulation and experimental results are successfully verified on the hardware prototype of the ball-beam system. Finally, this study provides dynamic performance with position accuracy and precision for the ball-beam control system.

References

1. Hirsch, R. (1999). Mechatronic instructional systems ball on beam system. *Shandor Motion Systems.*
2. Rosales, E.A. (2004). A ball-on-beam project kit. *Department of Mechanical Engineering, Massachusetts Institute of Technology.*
3. Lieberman, J. (2004). A robotic ball balancing beam. *MIT Media Lab Publications.*
4. Quanser (2006). The ball and beam module. Retrieved September 3, 2006, from http://www.quanser.com/products/ball_beam.
5. Eaton, P.H.; Prokhorov, D.V.; and Wunsch II, D.C. (2000). Neurocontroller alternatives for fuzzy ball and beam systems with nonuniform nonlinear friction. *IEEE Transactions on Neural Networks and Learning Systems*, 11(2), 423-435.
6. Ezzabi, A.A.; Cheok, K.C.; and Alazabi, F.A. (2013). A nonlinear backstepping control design for ball and beam system. *IEEE International Midwest Symposium on Circuits and System,* 56, 1318-1321.
7. Pang, Z.H.; Zheng, G.; and Luo, C.X. (2011). Augmented State Estimation and LQR Control for Ball and Beam System. *IEEE Conference on Industrial Electronics and Applications,* 1328-1332.
8. Yu, W.; and Ortiz, F. (2005). Stability analysis of PD regulation for ball and beam system. *IEEE Conference on Control Application*, 517-522.
9. Doyle, J.C.; Glover, K.; Khargonrkar, P.P.; and Francis, B.A. (1988). State space solution to standard H_2 and H control problem. *IEEE Trans. Automatic Control,* 34, 831-847.
10. Doyle, J.C.; and Stein, G. (1981). Multivariable feedback design: concept for classical/modern synthesis, *IEEE Trans. Automatic Control*, 26, 4-16.
11. Keshmiri, M.; Jahromi, A.F.; Mohebbi, A.; Amoozgar, M.H.; and Xie, F.W. (2012). Modeling and control of ball and beam system using model based and non-model based control approaches. *International Journal on Smart Sensing and Intelligent Systems,* 5(1), 14-35.
12. Pang, Z.H.; Zheng, G.; and Luo, C.X. (2011). Augmented state estimation and LQR control for ball and beam system. *IEEE Conference on Industrial Electronics and Applications*, 1328-1332.